REVISITING THE OBSERVABILITY OF THE $\boldsymbol{WH}$ AND $\boldsymbol{ZH}$, $\boldsymbol{H \to b\bar{b}}$ CHANNEL IN 14 TeV $\boldsymbol{pp}$ AND 2 TeV $\boldsymbol{p\bar{p}}$ COLLISIONS ($\boldsymbol{\ell b\bar{b}}$ AND $\boldsymbol{\ell\ell b\bar{b}}$ FINAL STATES)*

Elżbieta Richter-Wąs

Institute of Computer Science, Jagellonian University
Institute of Nuclear Physics
Kawiory 26a, 30-055 Cracow, Poland
CERN, EP Division, 1211 Geneva 23, Switzerland

(Received August 1, 2000)

A detailed study of the associated Standard Model Higgs boson production in 14 TeV pp (LHC) and 2 TeV $p\bar{p}$ (Tevatron) collisions, WH with $W \to \ell\nu$ and ZH with $Z \to \ell\ell$, with Higgs boson decays to $b\bar{b}$ pair, is presented for Higgs masses of 100 and 120 GeV. Presently, WH with $H \to b\bar{b}$ production is considered to be less promising than the $t\bar{t}H$ associated production for the Higgs searches at LHC. However, studies of Higgs searches at Tevatron indicate that this channel in combination with the WH/ZH channels leading to the $E_{\mathrm{T}}^{\mathrm{miss}} + b\bar{b}$ signature, offers good discovery potential in the mass range 90–140 GeV. The aim of this paper is to provide several details which lead to a quantitative comparison in a consistent framework of the physics potential for these channels in both colliding scenarios. The emphasis is put on the differences in the expected signal and background rates and compositions of the backgrounds.

PACS numbers: 14.80.Bn, 14.80.Cp, 14.65.Ha

* Supported in part by the Polish State Committee grant KBN 2P03B11819, by Polish–American Maria Skłodowska-Curie Joint Fund II in cooperation with PAA and DOE under project PAA/DOE-97-316 and Polish–French Collaboration with IN2P3.

CONTENTS

1. Introduction

If the mass of the Standard Model Higgs boson is lighter than $2m_W$, the $H \to b\bar{b}$ decay mode is dominant with a branching ratio of $\sim 90\%$. The observation of such a characteristic signature would be important for both the Higgs boson discovery and for the determination of the nature of any resonance observed in this mass region. Since the direct production, $gg \to H$ with $H \to b\bar{b}$, cannot be efficiently triggered nor extracted above the huge QCD two-jet background, the associated production with a W- or Z-boson or a $t\bar{t}$ pair remains as the only possible way to observe a signal from $H \to b\bar{b}$ decays. The leptonic decays of the W- or Z-boson provide an isolated high-p_{T} lepton for triggering and for rejection of the QCD background. The Higgs boson signal will be reconstructed as a peak in the invariant mass spectrum of tagged b-jets.

Prospects for the observability of the WH channel leading to the $\ell b\bar{b}$ signature, which is revisited in this paper, have already been considered in several documents of the ATLAS Collaboration [1, 3, 4]. It has been emphasized there that the expected sensitivity is rather weak, below 3σ, for an integrated luminosity of 30 fb^{-1}, for a Higgs mass in the range 100–120 GeV. The background to this signature is a mixture of the resonant WZ background, continuum backgrounds from $t\bar{t}$, $Wb\bar{b}$ and from the reducible Wjj background. The extraction of the signal itself will be very difficult given the presence of the resonant WZ background, the magnitude of the continuous background and the uncertainty related to the knowledge of its shape.

ZH production has not been considered in details so far by the ATLAS Collaboration for the reasons explained in [1]. With $Z \to \ell\ell$ decay leading to the $\ell\ell b\bar{b}$ signature, it would provide initial rates about six times lower than the WH channel and the signal-to-background ratio is not expected to be significantly larger with respect to that channel.

Given the fact that neither of these channels are considered as discovery channels at LHC, an attempt has been made to understand the reasons why they are claimed promising at the upgraded Tevatron [2]. Although some clear advantages come from the reduced center-of-mass energy (more central events than at LHC, much smaller $t\bar{t}$ cross-section), the expected rates should be substantially lower at the Tevatron than at the LHC for the same integrated luminosity.

In this paper, WH/ZH production giving rise to final states with accompanying two b-jets, is revisited once again for the LHC environment and for mass values $m_H = 100$ GeV and 120 GeV. Then a detailed comparison of the 2 TeV $p\bar{p}$ scenario versus the 14 TeV pp scenario is presented. An attempt is also made to break down, for signal and the dominant backgrounds, the differences between the acceptances reported in [2] and those obtained in this study.

Similar studies for ZH/WH production with the final state signature of b-jets plus missing transverse energy are presented in [5].

2. Observability of the $\ell b\bar{b}$ final state

2.1. Expected production rates

Table I shows the production cross-sections of the signal and the backgrounds for pp collisions at $\sqrt{s}$ = 14 TeV and $p\bar{p}$ collisions at $\sqrt{s}$ = 2 TeV. The $H, Z \to b\bar{b}$ and $W \to \ell\nu(\ell = e, \mu)$ branching ratios are included. The cross-sections for the W+jet production are quoted for the hard processes $q\bar{q} \to Wg$ and $qg \to Wq$, generated with the transverse momenta in the specified ranges. The Pythia5.7 Monte Carlo and CTEQ2L structure functions were used in the simulation.

TABLE I

Production cross-sections for WH signal and background processes for 14 TeV pp and 2 TeV $p\bar{p}$ collisions. The $H, Z \to b\bar{b}$ and $W \to \ell\nu(\ell = e, \mu)$ branching ratios are included.

Process	pp at 14 TeV σ [pb]	$p\bar{p}$ at 2 TeV σ [pb]	Ratio
WH, m_H = 100 GeV	0.40	0.042	10
WH, m_H = 120 GeV	0.21	0.020	10
WZ	0.86	0.083	10
$q\bar{q} \to W^* \to t\bar{b}$	1.0	0.11	10
$t\bar{t}$	228	2.62	87
$qg \to tq$	44.4	0.56	78
W+ jet			
p_T^{hard} = 10–30 GeV	1.1×10^4	9.7×10^2	11
p_T^{hard} = 30–50 GeV	2.7×10^3	1.7×10^2	16
p_T^{hard} = 50–100 GeV	1.5×10^3	7.4×10^1	20
p_T^{hard} = 100–200 GeV	3.2×10^2	8.3×10^0	38
p_T^{hard} > 200 GeV	3.5×10^1	0.3×10^0	117

The dominant uncertainties on the expected rates arise from higher-order corrections and from structure function parametrisation. The expected cross-sections differ by no more than 20% if CTEQ2L or CTEQ4L structure functions are used. A large uncertainty is expected for the estimated cross-section of the Wjj final state, due to the known limitations of the parton shower approach for the simulation of multijet final states.

For 14 TeV pp collision the expected rates for the signal and the resonant background are higher by a factor of 10 while for single and double $t\bar{t}$ production by a factor 80–90. The ratio of the cross-sections for $W+$ jet rises with the threshold on the transverse momenta of the hard process, varying from being ~ 10 for $p_{\mathrm{T}}^{\mathrm{hard}} = 10$–$30$ GeV to ~ 130 for $p_{\mathrm{T}}^{\mathrm{hard}} > 200$ GeV.

The Monte Carlo statistics used in this study is rather high: typically 5×10^5 events were simulated for each of the background processes while for the $W+$ jet process samples of 5×10^6 events were simulated in each $p_{\mathrm{T}}^{\mathrm{hard}}$ range.

2.2. Simulation procedure and selection criteria

The signal final state consists of a lepton from W decay, which triggers the experiment, and a pair of b-tagged jets which gives a peak in the invariant mass distribution.

The main ingredients of the reconstruction and selection procedure are:

- Efficiency for the lepton reconstruction, isolation and p_{T} threshold.
- Jet reconstruction efficiency, threshold on the jet transverse momenta and expected mass resolution;
- Jet-veto efficiency and threshold on the transverse momenta;
- Efficiency for b-jets tagging and non b-jets rejection.

The generated events, including QCD initial and final state radiation, fragmentation, hadronisation and decays, were simulated with a fast simulation of the ATLAS detector [6]. The following selection procedure was used:

- Electrons and muons were required to have transverse momenta larger than 20 GeV and to be in the pseudorapidity region $|\eta| < 2.5$. A 90% efficiency for lepton reconstruction was assumed. The isolation criteria are satisfied by most of the leptons from W decays. Events with a second lepton with $p_{\mathrm{T}} > 6$ GeV and $|\eta| < 2.5$ where rejected. This selection reduces to a negligible level the Zjj and Zbb backgrounds and reject also part of the $t\bar{t}$ background.

- Jets were reconstructed in a cone of $\Delta R = 0.4$ and were required to have transverse momenta above 10 GeV. The threshold on the transverse momenta as low as 10 GeV is used for the jets reconstruction in the cone[1] of $\Delta R = 0.4$. The reconstruction threshold for the fast simulation was defined at 5 GeV with assumed 100% efficient reconstruction of the calorimetric energy depositions and at 10 GeV after applying a Gaussian smearing with a $50\%/\sqrt{E}$ resolution [7]. This corresponds to a 15–18 GeV threshold on the recalibrated jet energies.

- b-tagging will be possible in ATLAS in the pseudorapidity range $|\eta| < 2.5$. A b-tagging efficiency of 60% for b-labelled jets with rejection against c-jets of 10 and against light jets of 100 is assumed [8]. The impact of the $p_{\rm T}$ and η dependence of the non-b-jets rejection for a constant b-tagging efficiency has been studied, [14], and has been shown to be small in terms of signal significance and signal-to-background ratio.

- Events with additional jets in the pseudorapidity range $|\eta| < 5.0$ and $p_{\rm T} > 15$ GeV or $p_{\rm T} > 30$ GeV are rejected.

After calorimeter reconstruction, the peak position of the m_{bb} distribution for the resonant WH and WZ events is shifted systematically by ~ 20 GeV towards lower values. The mass resolution is $\sim 10\%$. To recalibrate the jet energy scale a rather simple procedure is adopted to recover the out-of-cone energy loss due to fragmentation and hadronisation effects and to the expected response of the detector. Only the jet energy scale is calibrated without additional tuning of the mass energy scale. With the simplified procedure applied here, a precision of 1–2 % on the reconstructed mass energy scale is achieved over the mass range 80–140 GeV and a precision of better than 5% for the mass region down to 40 GeV. This was obtained with fast simulation and for both non-b and b-jets. Such a precision is adequate for the purpose of the studies presented here and allows control of the background shape well outside the mass region of the Higgs peak. Fig. 1 shows, the $(p_{\rm T}^{b-{\rm jet}}/p_{\rm T}^{b-{\rm quark}})$ distribution, after applying recalibration procedure, for the signal sample of $H \to b\bar{b}$ events with $m_H = 100$ GeV and the calibration factor applied to b-jets and to light jets after reconstruction with the fast simulation.

[1] As this channel is considered primarily at low luminosity a reconstruction cone of $\Delta R = 0.7$ might be more optimal.

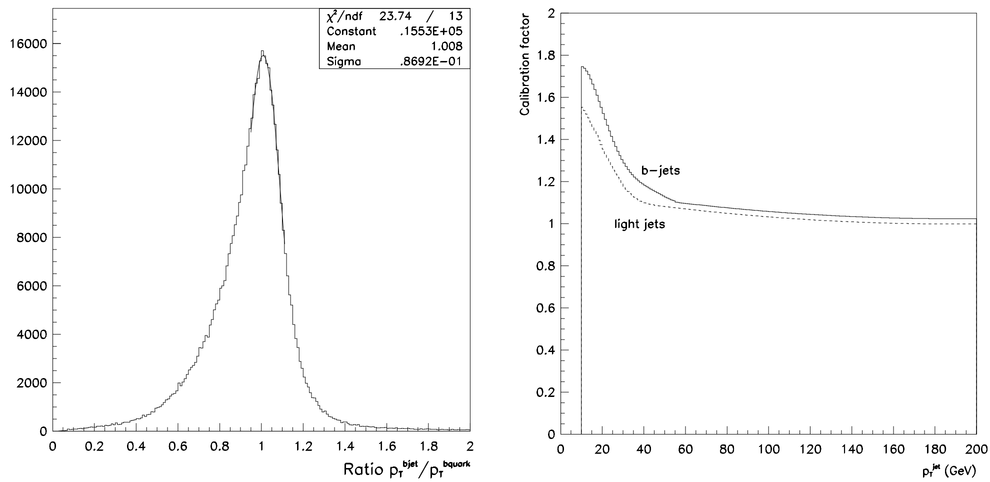

Fig. 1. The ($p_{\mathrm{T}}^{\mathrm{b-jet}}/p_{\mathrm{T}}^{\mathrm{b-parton}}$) distribution for recalibrated jets (left) and the calibration factor (right) applied to jets reconstructed with the fast simulation.

The final acceptance is sensitive to the threshold on the relatively tight jet veto which has to be imposed to suppress the $t\bar{t}$ background. Results are presented for two threshold values, 15 GeV and 30 GeV, both giving comparable signal significances with however different signal-to-background ratios and fractional background composition. Further optimisation of the thresholds for jet reconstruction and jet veto would be realistic only if performed with the full simulation of the detector and if complemented by more detailed studies of the Monte Carlo modelling of the hadronic activity in the event.

2.3. Signal and backgrounds in 14 TeV pp collisions

2.3.1. *WH* signal and *WZ* resonant background

Two mass points were simulated for the Higgs signal, m_H= 100 GeV and 120 GeV. Table II shows the expected cumulative acceptances for the kinematic selection criteria for the signal and the resonant background. Since the resolution obtained from the fast simulation is around 10% m_H, 100 $\pm$ 20 GeV and 120 $\pm$ 24 GeV mass windows were chosen to estimate the expected number of signal and background events for Higgs masses of 100 and 120 GeV respectively. The acceptances in the mass windows are given in Table III for the signal events and for the resonant background. Finally, the expected number of events for an integrated luminosity of 30 fb^{-1} is given in Table IV.

TABLE II

For the WH signal and WZ background events, expected cumulative acceptances of the kinematic selection criteria. Lepton identification and b-tagging efficiency are not included.

Cumulative acceptance	WH $m_H = 100$ GeV	WH $m_H = 120$ GeV	WZ $m_Z = 91$ GeV
Lepton	63.2%	66.0%	57.9%
+ 2 b-labelled jets	29.3%	33.1%	21.3 %
+ Jet veto 30 GeV	18.5%	18.8%	13.9 %
+ Jet veto 15 GeV	10.5%	10.6%	7.9 %

TABLE III

Acceptances in the respective mass windows (see text).

Acceptance in mass window	WH $m_H = 100$ GeV	WH $m_H = 120$ GeV	WZ $m_Z = 91$ GeV
	Jet veto 30 GeV		
$m_{bb} = 100 \pm 20$ GeV	84%	—	73%
$m_{bb} = 120 \pm 24$ GeV	—	85%	28%
	Jet veto 15 GeV		
$m_{bb} = 100 \pm 20$ GeV	89%	—	78%
$m_{bb} = 120 \pm 24$ GeV	—	90%	31%

The acceptance in the mass window 100 ± 20 GeV is of about 85% for WH signal events and 73% for the resonant WZ background. This can be considered as realistic, as an acceptance of 82% in the mass window 100 ± 20 GeV was obtained for signal events with full simulation [1] and for the selection without jet veto. A jet veto leads to a better acceptance inside the mass window, since events with abundant radiation do not pass this selection.

The kinematical acceptance for the resonant WZ channel is somewhat lower than for the WH signal and obviously lower is the acceptance in the respective mass windows. Nevertheless, the expected number of events from WZ production inside the mass windows is 40% higher than from the signal itself for the mass point $m_H = 100$ GeV and is comparable for $m_H = 120$ GeV. In practice the presence of a signal will broaden and distort the resonant peak from WZ events expected above a continuum background,

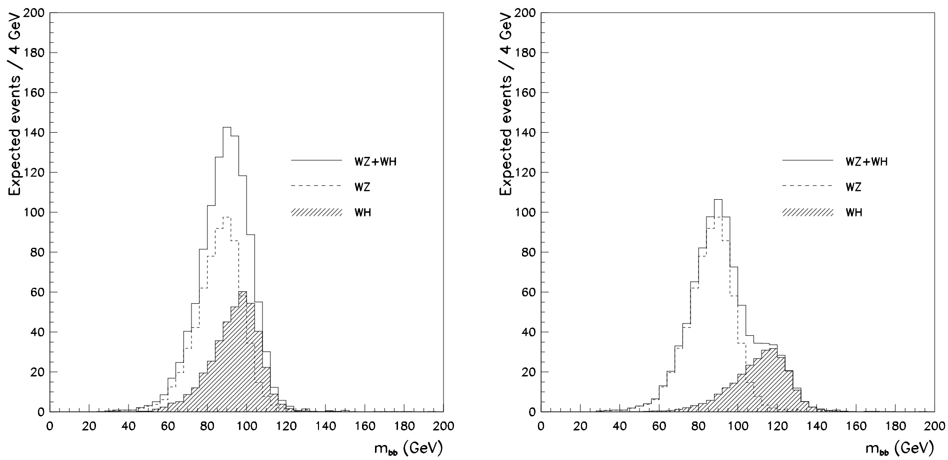

Fig. 2. The expected m_{bb} spectrum for WH (hatched), WZ (dashed) and $WH + WZ$ (solid) events for a Higgs mass of $m_H = 100$ GeV (left) and 120 GeV (right).

TABLE IV

For an integrated luminosity of 30 fb^{-1}, expected number of events from the WH signal and the WZ resonant background after all cuts, including lepton reconstruction and b-tagging efficiency.

Expected events	WH $m_H = 100$ GeV	WH $m_H = 120$ GeV	WZ $m_Z = 91$ GeV
	Jet veto 30 GeV		
$m_{bb} = 100 \pm 20$ GeV	605	—	845
$m_{bb} = 120 \pm 25$ GeV	—	325	325
	Jet veto 15 GeV		
$m_{bb} = 100 \pm 20$ GeV	360	—	520
$m_{bb} = 120 \pm 25$ GeV	—	195	207

as shown in Fig. 2. In the region close to the mass of the Z, the capability of extracting the signal peak would therefore relay on the knowledge of the WZ contribution which will be based on Monte Carlo simulation and data (*e.g.* $WZ \to l\nu ll$).

For Higgs masses above 100 GeV an asymmetric mass window would be more appropriate, as the contribution from the WZ background rises very fast when the lower bound of the mass window is moved below ~ 100 GeV.

2.3.2. Continuum background

• Wjj background

This background was simulated with the PYTHIA Monte Carlo, where jets in the final state come from the parton shower. The generation consisted of the tree level hard processes, $q\bar{q} \to Wg$ and $gq \to Wq$, accompanied by the initial and final state radiation. The total cross-section for W+jet events with $p_{\mathrm{T}}^{\mathrm{hard}} > 10$ GeV is 15 500 pb.

The contribution from the process $q\bar{q} \to Wg$ to the continuum irreducible $Wb\bar{b}$ background was also obtained from the exact matrix element (ME) calculations [9] implemented in to the HERWIG Monte Carlo (the same code as in [3] is used). The expected[2] cross-section times branching ratio for the $\ell b\bar{b}$ final state is 39.6 pb.

Table V shows the kinematic acceptance for inclusive Wjj events (both $q\bar{q}$ and qg contributions included) and separately for $q\bar{q} \to Wg$ events only. The acceptances are comparable in both samples. The heavy flavour composition of events accepted inside the mass window is given in Table VI. This composition is process dependent and is given for the inclusive $q\bar{q} \to Wg$, $qg \to Wq$ sample and for each subsample separately. It is found to be in good agreement with theoretical expectations discussed in [11]. A significantly lower fraction of cj, bc, cc and a higher fraction of $b\bar{b}$ events is found in the $q\bar{q} \to Wg$ sample than in the $gq \to Wq$ sample. It should be stressed, however, that the statistical error on numbers given in Table VI is quite large in some cases.

Direct comparison of the $q\bar{q} \to Wg$ process, see Table VII, simulated with the matrix element (ME) calculations and with the PYTHIA shower approach indicates that the predictions from PYTHIA are 20–30% lower. As the $q\bar{q} \to Wb\bar{b}$ matrix element for $2 \to 3$ process is fairly simple it should be well reproduced by the $2 \to 2$ process followed by gluon splitting. Nevertheless, this 20–30% discrepancy is much smaller than that obtained from *e.g.* comparing rates [12] for inclusive $W+$ 2jets and $W+$ 3jets production as given from PYTHIA and VECBOS. There, a factor of 1.8–2.0 was needed to bring PYTHIA results to these given by the matrix element calculations. In the $Wb\bar{b}$ case, however, the $b\bar{b}$ pair comes predominantly from gluon splitting of the leading gluon produced in the hard process $q\bar{q} \to Wg$. In addition, other possible effects like a softer multi-jet spectrum and/or enhanced heavy flavour content (for a discussion see [13]) could cancel each other, leading to a relatively small correction factor needed to bring the PYTHIA prediction for the $q\bar{q} \to Wg \to Wbb$ background in agreement with the ME calculations.

[2] For the $q\bar{q} \to Wb\bar{b}$ process the cross-section is lower than what was given in [3]. This difference comes from the fact that in Table 1 of [3] the total $pp \to Wb\bar{b}$ cross-section was given and a factor 1.75 was applied to the $q\bar{q} \to Wg \to Wb\bar{b}$ cross-section to account for the $gq \to Wq$ contribution.

The production cross-section for the $q\bar{q} \to Wg$ process is 40% of the total $pp \to Wq, Wg$ cross-section. On average, this 40% contribution holds also for the $Wb\bar{b}$ events selected after cuts. However, for any other flavour composition of jet the $q\bar{q}$ process contributes only 10–20% to the total number of expected events.

TABLE V

For Wjj events, expected cumulative acceptances of the kinematic selection criteria. For events generated with PYTHIA, these acceptances are given for samples (merged together) generated at different $p_{\rm T}^{\rm hard}$ bins and for events filtered by requiring 2 jets with $|\eta| < 2.5$.

Cumulative acceptance	$q\bar{q} \to Wg, qg \to Wq$ PYTHIA 5.7	$q\bar{q} \to Wg$ PYTHIA 5.7	$q\bar{q} \to Wbb$ ME + HERWIG 5.6.
Lepton	63.8%	63.0%	58.1%
+ 2 b-labelled jets	filter	filter	8.0%
+ jet veto 30 GeV	26.9%	29.1%	6.9%
+ jet veto 15 GeV	15.8%	14.8%	5.1%

TABLE VI

The heavy flavour composition of jj pairs accepted in the mass window after all kinematic cuts except the jet veto.

Fraction in mass window	$q\bar{q} \to Wg$, $qg \to Wq$	$q\bar{q} \to Wg$	$qg \to Wq$
bb	0.3%	0.5%	0.2%
bc	0.2%	0.2%	0.3%
cc	1.4%	0.8%	1.8%
jb	1.5%	1.5%	1.5%
jc	18.6%	10.7%	20.0%
jj	78.0%	86.3%	76.2%

For the final estimate of the Wjj background, see Table VIII, the results obtained from the PYTHIA are used without any corrections to the overall normalisation[3].

[3] A different approach was followed in [3] for the evaluation of the $Wb\bar{b}$ background. The ME + HERWIG prediction for $q\bar{q} \to Wb\bar{b}$ was used and the resulting cross-section was then multiplied by a factor 1.75 to take into account the contribution from the $gq \to Wq$ process.

TABLE VII

The same as Table IV but for $q\bar{q} \to Wb\bar{b}$ events.

Expected events	$q\bar{q} \to Wb\bar{b}$ PYTHIA 5.7	$q\bar{q} \to Wb\bar{b}$ ME + HERWIG 5.6.
	Jet veto 30 GeV	
m_{bb} = 100±20 GeV	3400	4200
m_{bb} = 120±24 GeV	2400	2900
	Jet veto 15 GeV	
m_{bb} = 100±20 GeV	2400	2900
m_{bb} = 120±24 GeV	1600	2000

TABLE VIII

The same as Table IV but for all Wjj events

Expected events	Wjj (bb) PYTHIA 5.7	Wjj (other) PYTHIA 5.7
	Jet veto 30 GeV	
m_{bb} = 100±20 GeV	9000	6400
m_{bb} = 120±24 GeV	7800	5300
	Jet veto 15 GeV	
m_{bb} = 100±20 GeV	4500	3200
m_{bb} = 120±24 GeV	3900	2600

• **Top pair and single top continuum background**

Top pair production contributes significantly to the continuum background. A non negligible background comes also from single top production. These backgrounds can be largely suppressed with a tight jet veto.

→ **Top pair production**

This channel results in a $WWb\bar{b}$ final state, with one W decaying into leptons and the other W decaying into leptons or jets. The lepton and jet vetos provide an overall rejection of ~ 100 against this channel (for a jet veto at 15 GeV), see Table IX. As already discussed in [3] a large fraction of the remaining background comes from $W \to \tau\nu$ events. This channel represents the second dominant source of background after Wjj. The expected number of events is given in Table X.

→ **Single top production: $W^* \to tb$**

Another source of irreducible $Wb\bar{b}$ background is a direct production of a off-mass shell $W^* \to tb$. In this case the HERWIG 5.6 Monte Carlo generator has been used, since this process is not available in PYTHIA. This channel has a production cross-section almost two orders of magnitude smaller than that of the inclusive $q\bar{q} \to Wb\bar{b}$ background. Although its acceptance is almost 3–5 times larger than that of $Wb\bar{b}$, it only increases the $q\bar{q} \to Wb\bar{b}$ background by $\sim$ 10–20%. The expected acceptances of the kinematic selection are given in Table IX, and the expected number of events after all cuts in Table X.

TABLE IX

For single top and top pair production, the expected cumulative acceptances of the kinematic selection criteria. For tb, tc events, the acceptances are given for events previously filtered by requiring two b- or c- jets.

Cumulative acceptance	$t\bar{t}$ PYTHIA 5.7	$W^* \to t\bar{b}$ HERWIG 5.6	tb, tc PYTHIA5.7
Lepton	68.2%	65.9%	74.7%
+ 2 b-labelled jets	40.6%	41.8%	filter
+ jet veto 30 GeV	1.8%	22.7%	2.5%
+ jet veto 15 GeV	0.4%	11.6%	0.8%

TABLE X

The same as Table IV but for single top and top pair production

Expected events	$t\bar{t}$ PYTHIA 5.7	$W^* \to t\bar{b}$ HERWIG 5.6	tb, tc PYTHIA 5.7
	Jet veto 30 GeV		
m_{bb} = 100±20 GeV	8450	580	250
m_{bb} = 120±24 GeV	10500	640	330
	Jet veto 15 GeV		
m_{bb} = 100±20 GeV	1900	300	80
m_{bb} = 120±24 GeV	2100	320	100

$\to$ **Single top production: tb, tc**

The acceptance for the b-jets selection for these channels is relatively low, in Table IX it is denoted as filtered and required that the $qg \to tq$ process was generated in several $p_{\mathrm{T}}^{\mathrm{hard}}$. In addition, an extra jet in the final state can be efficiently tagged, leading to a large rejection by the jet veto. The background from the continuum single top production turns out therefore to be significantly smaller than that from $t\bar{t}$ production.

2.3.3. Total signal and background

Tables XI and XII present the expected rates after all cuts for an integrated luminosity of 30 fb^{-1} for the WH signal with $m_H = 100$ GeV and 120 GeV and for the backgrounds. Results are given for two thresholds on the jet veto, 15 GeV and 30 GeV. Lepton reconstruction efficiency, b-tagging efficiency and mass window acceptance have been included in all rates. The mass window of ± 20 GeV (resp. ± 24 GeV) around the expected peak position of signal events is assumed for the Higgs masses 100 GeV (resp. 120 GeV).

TABLE XI

For an integrated luminosity of 30 fb^{-1}, the expected number of signal and background events for $m_H = 100$ GeV after all cuts.$B_{\rm other}$ denotes background contribution where one or both jets are misidentified as b-jets.

Process	Jet-veto 30 GeV	Jet-veto 15 GeV
WH	605	360
WZ	845	520
Wjj ($b\bar{b}$)	9000	4500
Wjj (other)	6400	3200
tt	8450	1900
$W^* \to tb$	580	300
tb, tc	250	80
Total bgd	25500	10500
$S/\sqrt{B}$	3.8	3.5
S/B	2.4%	3.4%
$B_{\rm other}/B_{\rm total}$	25%	30%

Neither the signal nor the backgrounds were rescaled to take into account higher-order corrections or limitations coming from the parton shower approach. In particular the contribution from $Wb\bar{b}$ events was taken from the simulation with PYTHIA.

So far only events where $W \to e\nu$ or $W \to \mu\nu$ were considered both for the signal and the backgrounds. Events giving rise to $\ell b\bar{b}$ final states could come also from WH, ZH events with $W \to \tau\nu$, $Z \to \ell\ell$ or $Z \to \tau\tau$ for a signal and respectively from ZZ, Z+jet for the background. The total signal rates can be increased by 13%, the irreducible resonant background by 20% while the non resonant background can be increased by up to 13% of the contribution coming from events with $W \to e\nu, \mu\nu$ only. These might lead to an improvement in the expected significance by at most 6%.

TABLE XII

The same as Table XI but for $m_H = 120$ GeV.

Process	Jet-veto 30 GeV	Jet-veto 15 GeV
WH	325	195
WZ	325	207
Wjj ($b\bar{b}$)	7800	3900
Wjj (other)	5300	2600
tt	10500	2100
$W^* \to tb$	640	320
$tb,\ tc$	330	100
Total bgd	24900	9250
$S/\sqrt{B}$	2.1	2.0
S/B	1.3%	2.1%
$B_{\text{other}}/B_{\text{total}}$	21%	28%

The general conclusions which can be driven from these results are:

- The expected signal significance, measured as $S/\sqrt{B}$, varies between 3.8 and 3.5 for $m_H = 100$ GeV, and between 2.1–2.0 for $m_H = 120$ GeV, depending on the jet veto threshold.
- The signal-to-background ratio is below 4% and the ratio of the reducible-to-irreducible background varies between 20–30%.
- A jet veto of 15-30 GeV is crucial to suppress the otherwise overwhelming $t\bar{t}$ background. Therefore this channel is expected to be difficult at high luminosity.
- The observation of the resonant WZ peak seems possible with a significance exceeding 5σ for an integrated luminosity of 30 fb^{-1}.

Fig. 3 shows the expected signal plus background mass distributions for $m_H = 100$ GeV and $m_H = 120$ GeV. Also shown is the background shape for the two dominant sources, Wjj and $t\bar{t}$.

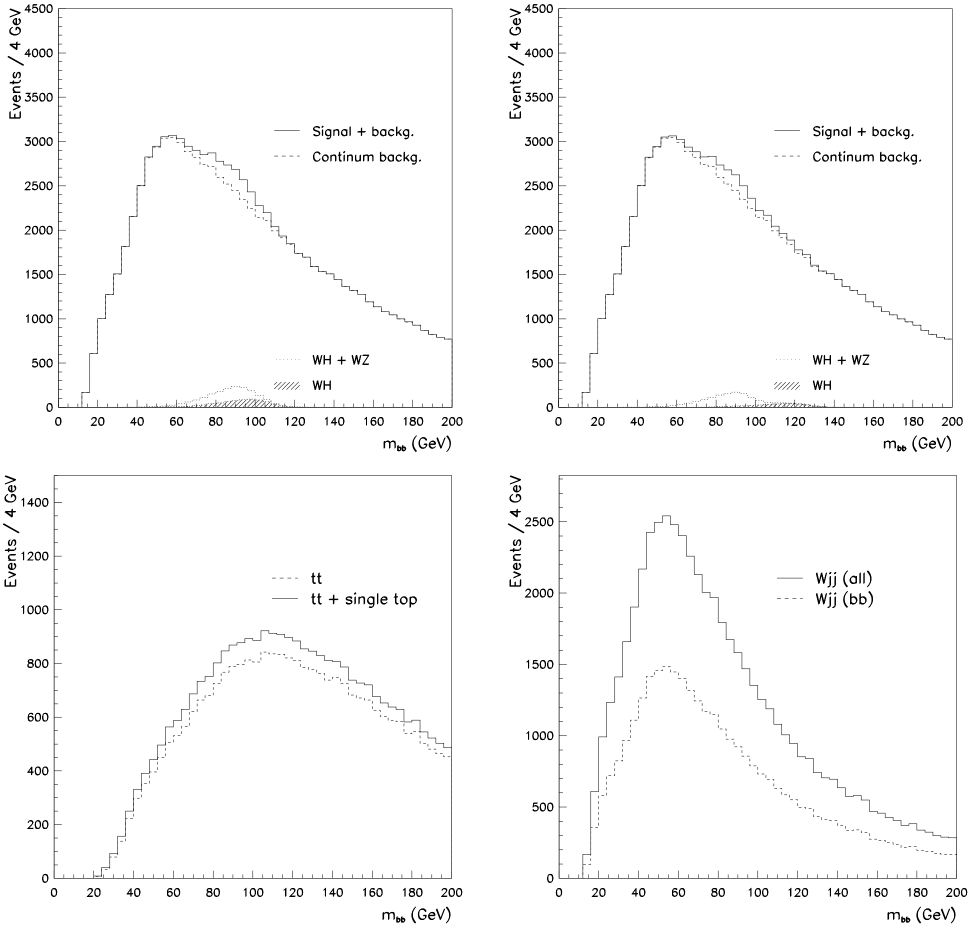

Fig. 3. Top: The expected m_{bb} distributions for signal plus background (solid line) for a Higgs mass of 100 GeV (left) and 120 GeV (right). The plots are normalised to the expected number of events for an integrated luminosity of 30 fb^{-1} and for jet veto at 30 GeV. The continuum background (dashed), the resonant signal+background (dotted) and the signal alone (hatched) are also shown. Bottom: The expected m_{bb} distributions for the top and the Wjj backgrounds for a jet veto at 30 GeV and for an integrated luminosity of 30 fb^{-1}.

2.4. 2 TeV $p\bar{p}$ versus 14 TeV pp

2.4.1. Introduction

The primary aim of this comparison is to study differences in the expected signal and background rates for 14 TeV pp and 2 TeV $p\bar{p}$ collisions, assuming comparable performance of the detectors, namely efficiencies for jets and lepton reconstruction, b-jet tagging and jet veto. Consistently the fast simulation of the ATLAS detector is used.

The following selection criteria are adopted:

- For the cases called (1) and (2) the ATLAS rapidity coverage and selection criteria are used with a jet-veto threshold at 30 GeV. Differences in the acceptances and expected rates are therefore directly related to differences in the physics (cross-sections) and kinematic features of events, etc.
- For the case called (3) a reduced geometrical coverage and slightly different selection criteria are used, following what specified in the Tevatron report [2]:
  - one lepton with $p_{\mathrm{T}} > 20$ GeV, no other leptons with $p_{\mathrm{T}} > 10$ GeV;
  - the detector coverage for b-tagging and lepton reconstruction is $|\eta| < 2.0$;
  - events with additional jets over $|\eta| < 2.5$ and $p_{\mathrm{T}} > 30$ GeV are rejected
- For the b-tagging performance, a 60% efficiency per b-labelled jet, for a rejection of 10 against c-jet and 100 against light jet is assumed.
- A lepton recosntruction efficiency of 90% is assumed for electrons and muons.
- A mass window of $\pm 2\sigma$ with $\sigma = 10\%$ m_H is used.

2.4.2. *WH* signal and *WZ* resonant background

The acceptance for signal events is higher almost by a factor of two for 2 TeV $p\bar{p}$ collisions than for 14 TeV pp collision. About 16% higher acceptance is expected for the request of an isolated lepton, about 19% for the request of a b-labelled pair and about 30% for the jet veto. The higher acceptance for the jet veto cut is caused mostly by the weaker QCD radiation at smaller centre-of-mass energy. The smaller geometrical acceptance of the Tevatron detectors is compensated by a softer jet-veto cut, as the $t\bar{t}$ background is much less severe at 2 TeV. Table XIII gives details on the expected acceptances.

Due to the smaller acceptance at 14 TeV, the expected signal rates are only by 5.3–5.5 times higher than at 2 TeV despite the fact that the initial cross-section is 10 times larger. Similarly, the acceptance for the resonant background is 2 times higher for 2 TeV $p\bar{p}$ collisions. About 17% higher acceptance is expected for the request of an isolated lepton, about 23% for the request of a b-labelled pair and about 28% for the jet-veto cut. Also in this case the higher acceptance for the jet veto is caused mostly by the smaller center-of-mass energy.

Due to, a smaller geometrical acceptance but a softer jet veto at the Tevatron, the expected rates for the resonant background are 5.7–6.0 times larger at LHC.

Table XIV gives details on the expected number of events for signal and resonant background.

TABLE XIII

For WH and WZ events, expected cumulative acceptances of the selection criteria. Lepton identification and b-tagging efficiencies are not included.

Cumulative acceptance	14 TeV pp (1)	2 TeV $p\bar{p}$ (2)	2 TeV $p\bar{p}$ (reduced) (3)	Ratio (1)/(3)
	WH, m_H = 100 GeV			
Lepton	63.2%	75.5%	73.5%	0.86
+ 2 b-labelled jets	29.3%	45.1%	40.9%	0.72
+ jet veto 30 GeV	18.5%	37.1%	33.6%	0.55
	WH, m_H = 120 GeV			
Lepton	66.0%	77.4%	75.6%	0.87
+ 2 b-labelled jets	33.1%	51.1%	49.3%	0.67
+ jet veto 30 GeV	18.8%	40.7%	36.7%	0.51
	WZ, m_Z = 91 GeV			
Lepton	57.9%	72.5%	68.0%	0.85
+ 2 b-labelled jets	21.3%	37.7%	31.0%	0.69
+ jet veto 30 GeV	13.9%	31.7%	25.9%	0.54

TABLE XIV

For an integrated luminosity of 30 fb^{-1}, expected number of events from the WH signal and the WZ background after all cuts. Lepton reconstruction efficiency, b-tagging efficiency and acceptance inside the mass window are included.

	14 TeV pp (1)	2 TeV $p\bar{p}$ (2)	2 TeV $p\bar{p}$ (reduced) (3)	Ratio (1)/(3)
	$m_H = 100$ GeV			
WH	605	127	115	5.3
WZ	845	181	148	5.7
	$m_H = 120$ GeV			
WH	325	65	59	5.5
WZ	325	67	54	6.0

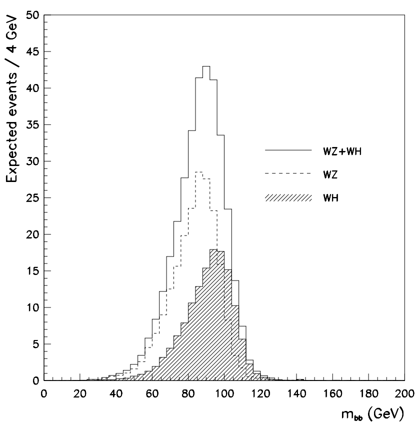

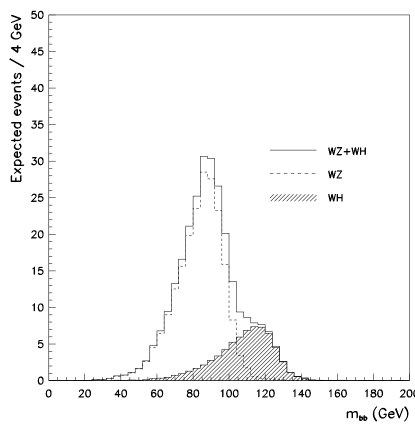

Fig. 4. The expected m_{bb} spectrum for WH (hached), WZ (dashed) and WH+WZ (solid) events for a Higgs mass $m_H = 100$ GeV (left) and 120 GeV (right).

2.4.3. Continuum background

The total continuum background is about 20 times higher in the 14 TeV pp scenario. For details on the acceptances see Table XV.

• ***Wjj* background**

As above the total acceptances for the kinematic cuts, (see Table XV), is smaller in the 14 TeV pp scenario. In this particular case the total acceptance is lower by a factor 1.6.

TABLE XV

For the continuum background, the expected acceptances of the selection criteria. Lepton reconstruction and b-tagging efficiencies are not included. For Wjj events the acceptances are given for samples generated with different $p_T^{\rm hard}$ bins (merged together). For single top production, tb and tc events, the acceptances are given for events previously filtered by requiring two b- or c- jets.

Cumulative acceptance	14 TeV pp (1)	2 TeV $p\bar{p}$ (2)	2 TeV $p\bar{p}$ (reduced) (3)	Ratio (1)/(3)
	Wjj			
Lepton	63.0%	78.7%	76.2%	0.83
+ 2 b-labelled jets	filter	filter	filter	—
+ jet veto 30 GeV	29.1%	53.9%	46.4%	0.63
	$t\bar{t}$			
Lepton	68.2%	73.1%	71.6%	0.95
+ 2 b-labelled jets	40.6%	45.3%	42.6%	0.95
+ jet veto 30 GeV	1.8%	4.2%	4.0%	0.45
	$W^* \to tb$			
Lepton	65.9%	80.0%	77.3%	0.85
+ 2 b-labelled jets	41.8%	57.4%	51.6%	0.81
+ jet veto 30 GeV	22.7%	43.9%	39.5%	0.57
	Single top tb, tc			
Lepton	74.7%	80.0%	77.8%	0.96
+ 2 b-labelled jets	filter	filter	filter	—
+ jet veto 30 GeV	2.5%	8.9%	7.2%	0.35

The total rate from Wjj events, after all cuts is 17–21 higher at LHC. The relative contribution from the reducible background Wjj(other) is 40% for 14 TeV pp collinsions and 20% for 2 TeV $p\bar{p}$ collisions.

• **$W^* \to tb$ background**

This background is of little importance in both scenarios. The total acceptance is much smaller at LHC but the expected rates are 4.7 times higher.

• **$t\bar{t}$ background**

The $t\bar{t}$ background is significantly smaller at 2 TeV because the cross section is almost 100 times smaller. This background is strongly suppressed with the jet veto cut. At 2 TeV such a jet veto is almost a factor of 3 less efficient as the smaller QCD radiation, and the jet-veto threshold (case 3) is slightly softer. The resulting acceptance is almost 2 times smaller at LHC and therefore the expected background rates 33 times larger.

• ***tb*, *tc* background**

Similar observations as for the $t\bar{t}$ channel are also valid in this case. The overall acceptance for the background is 3 times smaller at LHC, but the absolute event rate is 18–25 times higher.

2.4.4. Total signal and background

Tables XVI and XVII compare the expected signal and background rates for the 14 TeV pp scenario and the 2 TeV $p\bar{p}$ scenario for two mass points, $m_H = 100$ GeV and 120 GeV, and for a jet-veto cut of 30 GeV. Assuming the same detector performance, the signal and resonant background are a factor of 5 larger at LHC and the continuum background a factor 20 larger. The ratio of reducible to irreducible background is a factor 1.6–1.9 higher at LHC and the signal to background a factor of almost 3–5 smaller.

TABLE XVI

For an integrated luminosity of 30 fb^{-1}, the expected number of signal and background events for $m_H = 100$ GeV, after all cuts. Acceptance in the mass window, lepton reconstruction efficiency and b-tagging efficiency are included.

Process	14 TeV pp (1)	2 TeV $p\bar{p}$ (2)	2 TeV $p\bar{p}$ (reduced) (3)	Ratio (1)/(3)
WH	605	127	115	5.3
WZ	845	180	150	5.7
Wjj ($b\bar{b}$)	9000	840	710	13
Wjj (other)	6400	230	190	34
tt	8450	270	250	34
$W^* \to tb$	580	140	120	4.8
$tb,\ tc$	250	15	14	18
Total bgd	25500	1700	1450	18
$S/\sqrt{B}$	3.8	3.1	3.0	1.3
S/B	2.4%	7.5%	7.9%	0.3
$B_{\rm other}/B_{total}$	25%	14%	13%	1.9

The sensitivity in terms of $S/\sqrt{B}$ is higher by a factor 1.3 times larger at LHC, however, the environment is much more difficult. The background is not dominated by a single source, but is a combination of the W and $t\bar{t}$ events and a substantial contribution from the reducible Wjj. The ratio of the reducible to irreducible background is larger therefore a very good rejection of non-b jets is important. The $t\bar{t}$ background is potentially overwhelming and can be suppressed only with very tight jet-veto cuts. The feasibility and the efficiency of a tight jet-veto is crucial for the observation of this channel.

TABLE XVII

The same as Table XVI but for m_H = 120 GeV.

Process	14 TeV pp (1)	2 TeV $p\bar{p}$ (2)	2 TeV $p\bar{p}$ (reduced) (3)	Ratio (1)/(3)
WH	325	65	59	5.5
WZ	325	70	55	6
Wjj ($b\bar{b}$)	7800	550	470	17
Wjj (other)	5300	175	140	38
tt	10500	330	310	34
$W^* \to tb$	640	150	135	4.7
tb, tc	330	14	13	25
Total bgd	24900	1300	1100	22
$S/\sqrt{B}$	2.1	1.8	1.8	1.2
S/B	1.3%	5.0%	5.4%	0.2
$B_{\text{other}}/B_{\text{total}}$	21%	13%	13%	1.6

2.4.5. Comparison with the Tevatron report [2]

The results presented in the previous sections can be directly compared with those presented in the report of the Higgs Working Group of Tevatron [2]. Although [2] is not yet officially published, results from this report were publicly presented already several times [16], including recent presentation [17]. Therefore we consider them to be mature enough to justify performed below comparison. Two different analyses are presented in [2], based on the so called QFL and SHW simulations of the detector performance. The proposed selection criteria differ in some details between these two analyses, leading however to comparable signal significances in both cases.

In Tables XVIII–XXI comparisons between the results obtained with these studies and those reported in [2] are shown for mass point m_H= 110 GeV[4]. There are obvious differences in the assumptions concerning the expected detector performance. In the column labelled *This study*, the expected performance of the ATLAS detector at LHC is assumed, but the selection criteria are those proposed in [2]. This include a reduced pseudorapidity coverage and a softer jet veto, as already explained in Section 2.4.1 (case 3). In addition to the selection criteria described so far, a cut on the transverse missing energy, $E_{\mathrm{T}}^{\mathrm{miss}} > 20$ GeV is included[5] because it is used in the analysis presented in [2].

[4] Only for this mass point a complete break-down of the acceptance for signal and backgrounds is available in [2].

[5] This selection is used to suppress the possible background due to semileptonic decays inside QCD jets.

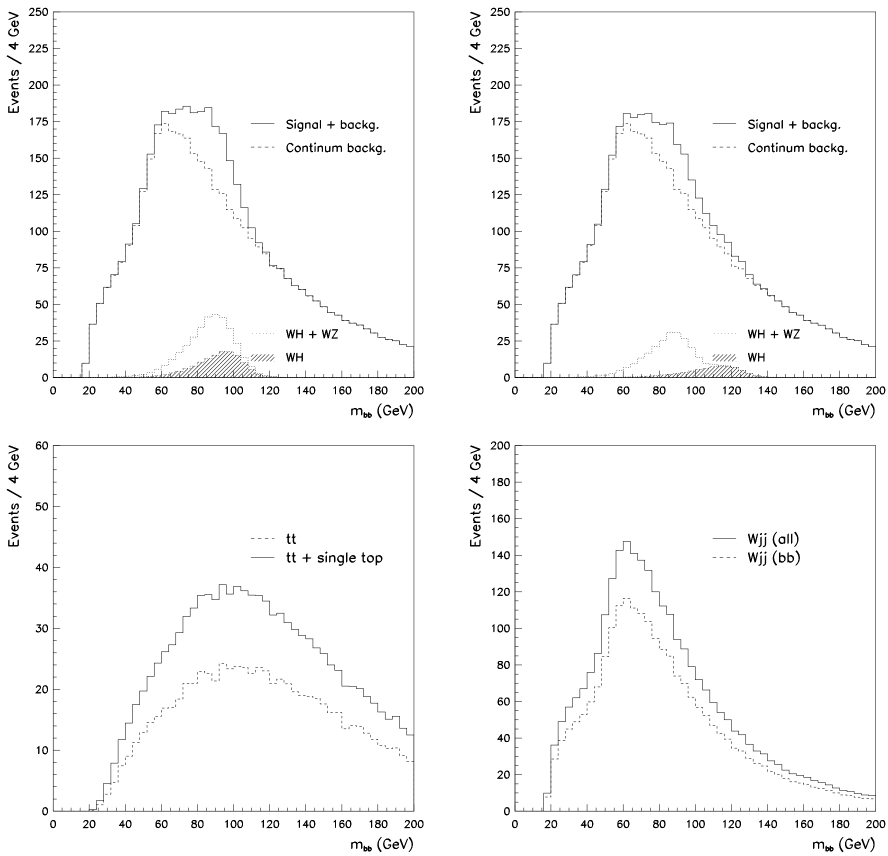

Fig. 5. Top: The expected m_{bb} distributions for the signal plus background (solid line) for a Higgs boson mass of 100 GeV (left) and 120 GeV (right) for 2 TeV $p\bar{p}$ collisions. A jet veto at 30 GeV is used and the plots are normalised to the expected number of events for an integrated luminosity of 30 fb^{-1}. Also shown are the distributions for the continuum background (dashed), resonant signal plus background (dotted) and signal only (hatched). Bottom: The expected m_{bb} distributions for the dominant continuum backgrounds for a jet veto of 30 GeV and for an integrated luminosity of 30 fb^{-1}.

The main ingredients of the detector performance, which are relevant for these Higgs searches are the b-tagging efficiency and the non-b jets rejection, as well as the efficiencies for jet reconstruction and jet veto. That is why shown are also results, denoted as *This study scaled*, obtained after rescaling[6] signal and background rates by the ratio of signal acceptances for double b-

[6] We could not used directly parametrisation for the b-tagging efficiency given in [2], as the information on the reconstruction efficiency for b-labelled pair was not available there.

tag respective for *This study* and *Tevatron report.* The column *This study scaled* shows results obtained by using the same acceptance for double b-tag for the signal events as that quoted in [2]. The background rates in this column are scaled with the same factor as for the signal.

Comparison with the *SHW* analysis

Selection criteria as close as possible to those of the SHW analysis have been applied in *This study* :

- *Lepton cut:* One isolated lepton with $p_{\rm T} > 20$ GeV and no additional with $p_{\rm T} > 10$ GeV, inside the rapidity coverage $|\eta| < 2.0$.
- $E_{\rm T}^{\rm miss}$ *cut:* The reconstructed missing transverse energy must be $E_{\rm T}^{\rm miss} > 20$ GeV. The calorimeter coverage extends up to 5.0 in pseudorapidity.
- *Double b-tag cut:* Two jets with $p_{\rm T} > 30$ GeV and 15 GeV respectively within $|\eta| < 2.0$ tagged as b-jets. A b-tagging efficiency of 60% per jet was used, with a rejection against c-jets of 10 and a rejection against light jets of 100. For *This study scaled*, the efficiency for double b-tag (including the jet reconstruction efficiency) is multiplied for both signal and background by a correction factor of 1.7.
- *Jet-veto cut:* Jets are reconstructed in the pseudorapidity range $|\eta| < 2.5$. No jets with $p_{\rm T} > 30$ GeV and not more than one jet with $p_{\rm T} > 15$ GeV are required.
- *Mass window cut:* A mass window of 110 ± 33 GeV, corresponding to $\sigma = 15\%\ m_H$, is used.

The discrepancy between (A) and (B) is roughly consistent with a factor 1.7 higher acceptance for double b-tag (including jets reconstruction) in (B), a factor 0.75 lower acceptance for jet veto in (B) and a factor 1.3 higher signal cross-section assumed in (B). After rescaling the rates for the double b-tag of the Tevatron study, the disagreement between (A') and (B) almost disappear, this agreement is however rather accidental for background rates.

A more detailed break-down of the differences between the two studies, which can be found below, supports these conclusions. This comparison should be treated with some caution as Table 5, 6 and 7 in Section C of [2] show some inconsistencies. In Tables XIX and XX, which give the break-down of acceptances, we quote the number of events estimated from the cross-sections (Table 5 of [2]) and acceptances (Table 6 of [2]) and these retrieved from Table 7 of [2]. They are not always consistent. As an example, the $t\bar{t}$ background estimate from Table 7 of [2] is 900 events while that from Tables 5 and 6 of [2] is 360 events.

TABLE XVIII

Comparison between "This study" (A), "This study scaled" (A'), see text, and Tevatron results (B) (numbers are taken from Table 7 in Section C of [2]). Expected number of events are compared for $m_H = 110$ GeV and for an integrated luminosity of 30 fb^{-1}. For consistency with original Tevatron studies $W \to \tau\nu$ is also included, but its contribution to the total signal and background is on the level of 3% only.

Process	This study (A)	This study scaled (A')	Tevatron report (SHW) Table 7 in [2] (B)	Ratio (A)/(B)	Ratio (A')/(B)
WH	85	144	150	0.6	1.0
WZ	140	240	330	0.4	0.7
Wjj ($b\bar{b}$)	1130	1920	1890	0.6	1.0
Wjj (other)	210	210	none	—	—
tt	350	590	900	0.4	0.6
single top	185	310	360	0.5	0.9
Total bgd	2015	3270	3510	0.6	0.9
$S/\sqrt{B}$	1.9	2.5	2.5	0.8	1.0
S/B	4.2%	4.4%	4.3%	1.0	1.0
$B_{\text{other}}/B_{\text{total}}$	10%	6.4%	none	—	—

Comparison with the *QFL* analysis

Selection criteria as close as possible to those of the QFL's analysis [2] have been applied in *This study*:

- *Lepton cut:* One isolated lepton with $p_{\rm T} > 20$ GeV and no additional with $p_{\rm T} > 10$ GeV, inside the rapidity coverage $|\eta| < 2.0$. Note that the isolated tracks from hadronic tau-decays are not considered in (A), but are included in (B)).

- $E_{\rm T}^{\rm miss}$ *cut:* The reconstructed missing transverse energy must be $E_{\rm T}^{\rm miss} > 20$ GeV. The calorimeter coverage extends up to 5.0 in pseudorapidity.

- The jet reconstruction threshold was set to 10 GeV.

- *Double b-tag cut:* Two jets with $p_{\rm T} > 30$ GeV and 15 GeV respectively within $|\eta| < 2.0$ tagged as b-jets. A b-tagging efficiency of 60% per jet was used, with a rejection against c-jets of 10 and a rejection against light jets of 100. For *This study scaled*, the efficiency for double b-tag (including the jet reconstruction efficiency) is multiplied for both signal and background by a correction factor of 1.3.

- *Jet-veto cut:* Jets are reconstructed in the pseudorapidity range $|\eta| < 2.4$. No jets with $p_{\rm T} > 20$ GeV.

TABLE XIX

Break-down of acceptances, and the expected number of events for the WH signal with 110 GeV and the WZ resonant background.

Process	This study (A)	Tevatron report (SHW) Table 5, 6 in [2] (B)	Comments
	WH signal		
σ (pb)	0.16	0.22	1.4 higher σ in (B)
BR	0.331×0.85	0.331×0.85	τ's from W included
Lepton	46.4%	39.6%	90% effic. included in (A)
$E_{\mathrm{T}}^{\mathrm{miss}}$	84.4%	89.0%	
Double b-tag	22.3%	37.8%	
Jet veto	75.8%	57.3%	
Mass window	94.5%	90.3%	
Total accept	6.25%	6.9%	
Total accept $\times$BR	1.76%	1.94%	1.1 higher accept. in (B)
Expected events	85	128 (accept.) 150 (Table 7 in [2])	1.5 higher rates in (B) 1.8 higher rates in (B)
	WZ background		
σ (pb)	2.5	3.2	1.3 higher in σ (B)
BR	$0.331 \cdot 0.15$	$0.331 \cdot 0.15$	τ's from W included
Lepton	42.5%	33.8%	90% effic. included in (A)
$E_{\mathrm{T}}^{\mathrm{miss}}$	86.0%	84.8%	
Double b-tag	16.7%	34.6%	
Jet veto	80.0%	64.8%	
Mass window	80.0%	84.2%	
Total accept	3.9%	5.4%	
Total accept $\times$BR	0.19%	0.27%	1.4 higher accept. in (B)
Expected events	140	260 (accept.) 330 (Table 7 in [2])	1.8 higher rates in (B) 2.3 higher rates in (B)

- *Mass window cut:* A mass window of 110 ± 22 GeV, corresponding to $\sigma = 10\%\ m_H$, is used for (A) and (A'). Results in (B) are given for mass window 91.8–123.3 GeV.

TABLE XX

The same as Table XIX but for the other background channels.

Process	This study (A)	Tevatron report (SHW) Table 2, 3 in [2] (B)	Comments
	$q\bar{q} \to Wbb$ background		
σ (pb)	49.3 (ME)	10.6	Cut on generation in (B)?
BR	0.331	0.331	τ's from W included
Lepton	46.0%	36.3%	τ's from W included
$E_{\mathrm{T}}^{\mathrm{miss}}$	90.0%	78.7%	90% effic. included in (A)
Double b-tag	2.6%	19.7%	
Jet veto	93.3%	98.2%	
Mass window	24.7%	28.1%	
Total accept	2.5%	1.56%	
Total accept $\times$BR	0.075%	0.52%	
Expected events	1130	1654 (accept.)	1.5 higher rates in (B)
		1890 (Table 7 in [2])	1.7 higher rates in (B)
	$t\bar{t}$ background		
σ (pb)	7.8	7.5	Comparable σ in (A), (B)
BR	0.552	0.552	τ's from W included
Lepton	44.7%	21.7%	90% effic. included in (A)
$E_{\mathrm{T}}^{\mathrm{miss}}$	85.7%	91.9%	
Double b-tag	23.0%	46.4%	
Jet veto	8.2%	7.9%	
Mass window	40.0%	39.6%	
Total accept	0.28%	0.29%	
Total accept $\times$BR	0.15%	0.16%	$\sim$ accept. in (A), (B)
Expected events	350	360 (accept.)	$\sim$ rates in (A), (B)
		900 (Table 7 in [2])	2.6 higher rates in (B)

One should notice, that the same number of signal events is expected from the SHW and QFL analyses, but the estimated backgrounds differ by a factor 2!

3. Observability of the $\ell\ell b\bar{b}$ final state

The channel is marginal for Higgs discovery at LHC. This is demonstrated by the study presented in this Section which was performed for a Higgs mass $m_H = 100$ GeV.

TABLE XXI

Expected number of signal ($m_{\rm H}$ = 110 GeV and background events after all cuts for "This study" (A), "This study scaled" (A') (see text) and Tevatron report (B) (numbers are from Table 4 in Section C of [2]).

Process	This study (A)	This study scaled (A')	Tevatron report (QFL) Table 4 in [2] (B)	Ratio (A)/(B)	Ratio (A')/(B)
WH	120	152	150	0.8	1.0
WZ	130	160	147	0.9	1.1
Wjj ($b\bar{b}$)	720	910	567	1.3	1.6
Wjj (other)	200	200	none	—	—
tt	210	260	366	0.6	0.7
single top	150	190	354	0.4	0.5
Total bgd	1410	1720	1434	1.0	1.2
$S/\sqrt{B}$	3.2	3.7	4.0	0.8	0.9
S/B	8.5%	8.8%	10.5%	0.8	0.7

The following selection criteria are applied:

- *2 leptons:* two opposite-sign, same-flavour leptons (OS-SF leptons) satisfying the following requirements:
  - one electron or muon with $p_{\rm T} > 20$ GeV or two electrons or muons with $p_{\rm T} > 15$ GeV inside $|\eta| < 2.5$;
  - the reconstructed di-lepton mass inside a mass window of $\pm$ 6 GeV around the Z mass.

  The lepton reconstruction efficiency is conservatively assumed to be 90% per lepton.

- *2 b-jets:* 2 b-labelled jets with reconstructed transverse momenta $p_{\rm T} > 15$ GeV and $|\eta| < 2.5$. A b-tagging efficiency of 60% with a rejection of 10 and 100 against c-jets and light-jets respectively is used.

- *Jet-veto:* events with additional jets with $p_{\rm T} > 30$ and $|\eta| < 5.0$ are rejected.

- *Mass window:* It is chosen to be 100 ± 20 GeV for $m_H = 100$ GeV, which corresponds to the resolution of 10% m_H .

3.1. Expected production rates

Table XXII shows the production cross-sections for the signal and the various backgrounds for 14 TeV pp and 2 TeV $p\bar{p}$ collisions. The $H, Z \to b\bar{b}$ and $Z \to \ell\nu(\ell = e, \mu)$ branching ratios are included. The cross-sections for Z+jet production are quoted for the hard processes, $q\bar{q} \to Zg$ and $qg \to Zq$, generated with the transverse momenta in the specified ranges.

TABLE XXII

Production cross-sections for the ZH signal and for backgrounds for 14 TeV pp and 2 TeV $p\bar{p}$. The $H, Z \to b\bar{b}$ and $Z \to \ell\ell$ ($\ell = e, \mu$) branching ratios are included.

Process	pp at 14 TeV $\sigma[pb]$	$p\bar{p}$ at 2 TeV $\sigma[pb]$	Ratio
$ZH, m_H = 100$ GeV	0.069	0.0072	10
ZZ	0.23	0.023	10
$t\bar{t}$	27.8	0.32	87
Z+jet			
$p_{\rm T}^{\rm hard} = 10$–30 GeV	2.2×10^3	2.3×10^2	10
$p_{\rm T}^{\rm hard} = 30$–50 GeV	3.8×10^2	2.6×10^1	14
$p_{\rm T}^{\rm hard} = 50$–100 GeV	2.0×10^2	1.0×10^1	20
$p_{\rm T}^{\rm hard} = 100$–200 GeV	4.3×10^1	1.2×10^0	35
$p_{\rm T}^{\rm hard} > 200$ GeV	4.9×10^0	4.9×10^{-2}	100

For the signal and the resonant ZZ background the cross-section is almost a factor of 10 higher at LHC energies. The Z+jet rates are also 10 times higher for a low $p_{\rm T}^{\rm hard}$ cut, but the ratio to the Tevatron rate increases with increasing transverse momenta of the hard scattering process. The expected production cross-section for the $t\bar{t}$ pairs is almost 100 times higher at LHC.

3.2. Signal and backgrounds in 14 TeV pp collisions

3.2.1. *ZH* signal and *ZZ* resonant background

The acceptance for signal events is 15% and 8.6% for jet-veto thresholds of 15 and 30 GeV (see Table XXIII). This does not include the b-tagging and lepton reconstruction efficiencies. This number is 20% lower than respectively for WH events with the $\ell b\bar{b}$ signature. The acceptance in the mass window is of 85%. The expected signal rates for an integrated luminosity of 30 fb^{-1} are given in Table XXIV. These rates are almost a factor of 10 lower than those expected from the $WH \to \ell bb$ channel (Table IV).

TABLE XXIII

Cumulative acceptances of the kinematic selection criteria for the ZH signal and the ZZ resonant background. Lepton reconstruction and b-tagging efficiencies are not included.

Cumulative acceptance	ZH	ZZ
2 leptons	54.6%	45.4%
+ 2 b-labelled jets	25.3%	16.7%
+ Jet veto 30 GeV	15.1%	11.0%
+ Jet veto 15 GeV	8.6%	6.2%

TABLE XXIV

For an integrated luminosity of 30 fb^{-1}, expected number of events from the ZH signal and the ZZ resonant background after all cuts.

Expected events	ZH	ZZ
No jet veto	115	230
Jet veto 30 GeV	80	160
Jet veto 15 GeV	45	100

The acceptance for the ZZ resonant background with one of the Z-bosons decaying into leptons ($Z \to \ell\ell$) and the second one into a $b\bar{b}$ pair ($Z \to b\bar{b}$) is smaller than for the ZH signal. Also smaller is the acceptance in the bb mass window. The expected number of events in the mass window is nevertheless 2 times larger than for the signal. It is a less favourable situation than that for the WH channel where the expected resonant background is only 40% higher than the signal. The presence of a Higgs signal will broaden and distort the mass peak expected from the resonant background, as shown in Fig. 6 for $m_H = 100$ GeV.

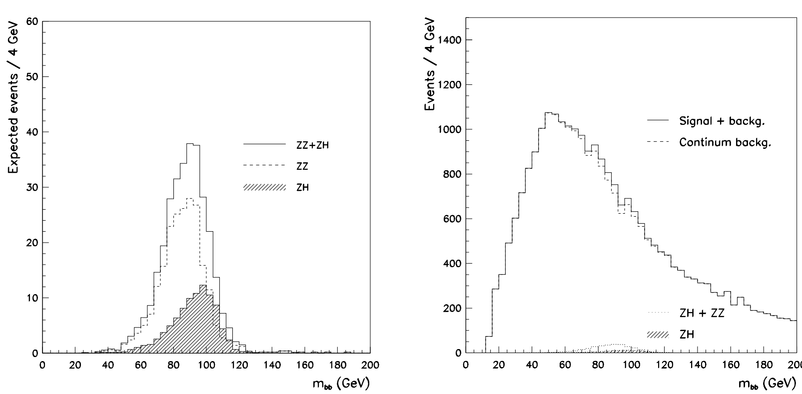

Fig. 6. The expected m_{bb} distribution signal and resonant background (left) and of total background and signal+background (right) for the jet-veto threshold 30 GeV and an integrated luminosity of 30 fb^{-1}.

3.2.2. Continuum background

Only Zjj and $t\bar{t}$ contribute significantly to the background to this channel. For details on the acceptances see Table XXV.

• **Top pair production.**

This channel gives rise to $\ell\ell b\bar{b}$ final states if both W's decays semileptonically. The acceptance for two OS–SF leptons with invariant mass within $\pm$ 6 GeV of the Z mass is 2.6%. On the other hand the jet veto is much less efficient than for $\ell b\bar{b}$ final states where the second W from the top-quark decays predominantly into hadrons. The total acceptance for $t\bar{t}$ production, normalised to a $t\bar{t} \to \ell\ell\nu\nu b\bar{b}$ sample, is 0.3%. The total background from $t\bar{t}$ events is a factor of 10–25 smaller, depending on the threshold of the jet-veto, than for the $\ell b\bar{b}$ channel.

• **Zjj continuum background**

This background was simulated with PYTHIA where multi-jets arise from parton shower. In PYTHIA, the tree level processes $qg \to qZ$ and $q\bar{q} \to gZ$ are available. The cross-section is dominated by the first one. It does not include, however, all tree level diagrams leading to the $Zb\bar{b}$ final state [15], namely the $b\bar{b}$ fusion *i.e.* $gg \to b\bar{b}Z$ subprocess is missing. Such configuration can be obtained only through initial state radiation. Therefore the total $Zb\bar{b}$ background as given by PYTHIA is underestimated [15]. On the other hand, the reducible Zjj background where at least one j is not b can not be simulated with the exact matrix from [15]. As in any case the signal ZH signal is marginal one, this rather crude estimate of the Zjj background is hopefully adequate for the evaluation presented below.

TABLE XXV

Cumulative acceptances of the selection criteria for the continuum $t\bar{t}$ and Zjj backgrounds. The Zjj events were filtered by asking 2 jets within $|\eta| < 2.5$. Lepton identification efficiency and b-tagging efficiency are not included.

Cumulative acceptance	Zjj	$t\bar{t}$
2 leptons	27.6%	2.6%
+ 2 b-labelled jets	filter	1.6%
+ Jet veto 30 GeV	8.4%	0.7%
+ Jet veto 15 GeV	4.3%	0.3%

As a consequence of the fact that different hard processes contribute to Zjj and Wjj production the jet flavour composition is very different in the two cases, see Table XXVI and Table VI. The fraction of $Zb\bar{b}$ events in the inclusive Zjj sample is 2.3% while the fraction of $Wb\bar{b}$ events in the inclusive Wjj sample is only 0.3%. The main difference comes from the fact that

TABLE XXVI

Composition of the jet flavour for the Zjj events accepted in the $b\bar{b}$ mass window (b-tagging not applied).

Fraction in mass window	$q\bar{q} \to Zg$, $qg \to Zq$	$q\bar{q} \to Zg$	$qg \to Zq$
bb	2.3%	0.5%	2.5%
bc	0.2%	0.2%	0.3%
cc	2.0%	0.9%	2.3%
jb	5.5%	5.3%	5.9%
jc	9.6%	9.0%	10.0%
jj	80.4%	84.1%	79.0%

$qg \to Zb$ production comes from the process $bg \to Zb$, which is accompanied by second spectator b-quark from the gluon splitting in the evolution of the structure functions. In this case the Zbb final state is relatively easy to happen. On the other hand $qg \to Wb$ scattering is very rare because it would require a top-quark in the initial state, picked-up from the evolved structure functions. As a consequence in the $qg \to Wq$ process one observes enhancement of the cj fraction with respect to what observed in the $qg \to Zq$ process. On the other hand, the flavour composition for the $q\bar{q} \to Zg$ and $q\bar{q} \to Wg$ processes is very similar since in both cases the $b\bar{b}$ pair arises from g splitting.

As a consequence, after b-jets identification, the background from the Zjj channel is dominated by $Z \to b\bar{b}$ events with two real b (90% of the total Zjj background) while for the Wjj channel the $Wb\bar{b}$ contribution amounts only to 60% of the total Wjj background.

TABLE XXVII

For an integrated luminosity of 30 fb^{-1}, expected number of events from the continuum Zjj and $t\bar{t}$ backgrounds after all cuts.

Expected events	Zjj (bb)	Zjj (other)	$t\bar{t}$
No jet veto	8300	700	850
Jet veto 30 GeV	6300	500	350
Jet veto 15 GeV	3300	350	175

3.2.3. Total signal and background

Table XXVIII presents the expected rates for the ZH signal and backgrounds giving $\ell\ell b\bar{b}$ final states for an integrated luminosity of 30 fb^{-1}. The efficiencies for leptons reconstruction and b-tagging have been included and a mass window of $\pm$ 20 GeV around the nominal Higgs mass, $m_H = 100$ GeV, is used. Neither the signal nor the backgrounds were rescaled to take into account higher-order corrections or limitations coming from the parton shower approach.

The sensitivity of this channel is found to be only marginal. Around 50 signal events over 4000 background events are expected. This gives a statistical significance below 1σ and a signal-to-background ratios of 1% only. The significance for the observation of the resonant $ZZ + ZH$ peak is 3.5σ. The ZH signal itself would contribute only 30% to the resonant peak in the $b\bar{b}$ mass window.

Given the fact that the dominant background is $Zb\bar{b}$, which has been simulated with PYTHIA, the estimates for $S/\sqrt{B}$ shown in Table XXVIII are on the optimistic side.

Figure 6 shows the expected m_{bb} distribution for the total background and for the signal plus background, for a jet-veto threshold of 30 GeV. This figure illustrates also that it will be hopeless an atempt to extract such a marginal signal given the shape and magnitude of the continuum background.

TABLE XXVIII

For an integrated luminosity of 30 fb^{-1}, expected number of signal and background events after all cuts.

Process	No jet-veto	Jet-veto 30 GeV	Jet-veto 15 GeV
ZH	115	80	45
ZZ	230	160	100
tt	850	350	150
Zjj (bb)	8300	6300	3300
Zjj (other)	700	500	350
Total bgd	10100	7300	3900
$S/\sqrt{B}$	1.1	0.9	0.7
S/B	1.1%	1.1%	1.1%

The expected sensitivity for the $\ell\ell b\bar{b}$ signature is much weaker than that for the $\ell b\bar{b}$ signature. For the selection with a jet-veto at 30 GeV, the expected signal rates are 8 times lower with the background rates are only 3.5 times lower in the $\ell\ell b\bar{b}$ case as compared to the $\ell b\bar{b}$ case. This leads to a facgor of ~ 4 smaller statistical significance. Although in the case of the $\ell\ell b\bar{b}$ channel the jet-veto can be relaxed or removed (the $t\bar{t}$ background is less severe) this would increase the signal and background rates by at most a factor of 2 and the statistical significance by at most 40%.

Also extracting a resonant ZZ peak in the $\ell\ell b\bar{b}$ channel is more difficult than extracting a WZ peak in the $\ell b\bar{b}$ channel.

As can be concluded from Table XXVIII the jet veto can be safely relaxed or abandoned since the $t\bar{t}$ background would not exceed 10% of the total background for the selection with no jet-veto. This should allow probing channel also at high luminosity. However, with presented analysis, even with the ultimate integrated luminosity of 300 fb^{-1} and a b-tagging efficiency of 50% the expected significance would be at the level of 3.0σ only.

3.3. 2 TeV $p\bar{p}$ versus 14 TeV pp

The $ZH \to \ell\ell\bar{b}$ is considered non-marginal for Higgs at the Tevatron [2]. To understand the differences in the expected physics potential for both colliding scenarios, a quantitative comparison has been performed and is presented below.

As in the previous studies for both colliding scenarios the ATLAS fast simulation program is used.

For the comparison presented below the following selection criteria were used consistently:

- We denote with (1) and (2) analyses based on the kinematical coverage of the ATLAS detector and on the selection criteria discussed in the previous sections. Differences in acceptances and expected rates are therefore directly related to the differences in physics.

- Results denoted with (3) were obtained with a geometrical coverage and selection criteria similar to those in [2].

  - two leptons with $p_{\mathrm{T}} > 10$ GeV inside the rapidity range $|\eta| < 2.0$ and with invariant mass in the window $m_Z \pm 6$ GeV.
  - b-tagging and lepton reconstruction over $|\eta| < 2.0$.
  - no additional jets with $p_{\mathrm{T}} > 30$ GeV, and no more than one jet with $p_{\mathrm{T}} > 15$ GeV within the pseudorapidity range $|\eta| < 2.5$.

- A b-tagging efficiency of 60% per b-labeled jet, with a rejection of 10 per c-jet and 100 per light-quark jet were used.

- A mass window of 100 ± 20 GeV.

- The lepton reconstruction efficiency is conservatively assumed to be 90% per lepton.

3.3.1. *ZH* signal and resonant background

The signal acceptance is 80% higher for the 2 TeV $p\bar{p}$ scenario. About 10% higher acceptance is expected for the request of a pair of isolated leptons, about 20 % for the request of a pair of b-labelled jets and about 40% for the jet-veto cut. The higher acceptance of the jet veto cut is due mostly to the smaller centre-of-mass energy resulting in a smaller QCD radiation. The smaller geometrical acceptance of the Tevatron detectors is compensated by the softer jet-veto cut (as the $t\bar{t}$ background is much smaller at 2 TeV $p\bar{p}$).

The smaller acceptance at LHC energies leads to expected signal rates which are only 5.7 times higher than at the Tevatron, despite 10 times larger initial cross-section.

The acceptance for the resonant background is comparable before jet-veto cuts are applied. Since the jet veto is more efficient at 14 TeV the final acceptance is 40% higher at 2 TeV (see Table XXIX).

TABLE XXIX

Expected cumulative acceptances of the selection criteria for ZH ($Z \to \ell\ell$) signal events. Lepton reconstruction and b-tagging efficiencies are not included.

Cumulative acceptance	14 TeV pp (1)	2 TeV $p\bar{p}$ (2)	2 TeV $p\bar{p}$ (reduced) (3)	Ratio (1)/(3)
	ZH			
2 leptons	54.6%	61.6%	60.2%	0.90
+ 2 b-labelled jets	25.3%	36.8%	33.5%	0.75
+ jet veto 30 GeV	15.1%	30.3%	27.5%	0.55
	ZZ			
2 leptons	45.4%	58.6%	50.7%	0.89
+ 2 b-labelled jets	16.7%	30.5%	23.1%	0.72
+ jet veto 30 GeV	11.0%	25.6%	19.3%	0.57

The expected rates after all cuts are given in Table XXX. The resonant background are 6.9 times higher at 14 TeV since the signal is only a factor 5.7 higher at 14 TeV. The signal to resonant background ratio is worse at 14 TeV.

TABLE XXX

For an integrated luminosity of 30 fb^{-1}, expected number of events from ZH signal and ZZ resonant background for a selection with a jet-veto 30 GeV. The numbers include the acceptance inside mass window, lepton reconstruction and b-tagging efficiencies.

Expected events	14 TeV pp (1)	2 TeV $p\bar{p}$ (2)	2 TeV $p\bar{p}$ (reduced) (3)	Ratio (1)/(3)
	ZH			
No jet-veto	115	20	18	6.4
Jet-veto 30 GeV	80	16	15	5.3
	ZZ			
No jet-veto	230	47	34	6.8
Jet-veto 30 GeV	160	28	23	6.9

3.3.2. Continuum background

- **Top pair production**

The $t\bar{t}$ background is less severe at 2 TeV. the cross-section is almost 100 times smaller than at 14 TeV. In the analysis performed here, this background is mostly suppressed by the tight mass window cut applied to the di-lepton pair. In addition, it can also be suppressed by the jet veto. For 2 TeV $p\bar{p}$ collisions such veto would be almost 3 times less efficient because of the smaller QCD radiation and because the dominant production mode is $q\bar{q} \to t\bar{t}$ and not $gg \to t\bar{t}$. The jet veto proposed in a 2 TeV environment is slightly softer. As a consequence the acceptance is almost a factor of 2 lower for the 14 TeV scenario and therefore the expected $t\bar{t}$ background is 30 times higher. This has to be compared with a 5.7 times higher signal.

- **Zjj continuum background**

As for the other channels, the acceptances for isolated leptons, double b-tag and jet-veto cuts, are lower in the 14 TeV scenario (Table XXXI). The total acceptance is almost a factor of 2.5 smaller.

However, this background does not simply scale with the acceptance and the cross-section. The fraction of jets with a heavy flavour content is much higher in the 14 TeV case, as illustrated in Table XXXII. Therefore the expected number of true $Zb\bar{b}$ events in the mass window is almost 30–50 times higher in the 14 TeV scenario despite the fact that the initial cross-section is only 10–15 times higher.

TABLE XXXI

Cumulative acceptances of the selection criteria for the $t\bar{t}$ and Zjj continuum backgrounds. The Zjj events were filtered by requiring 2 jets with $|\eta| < 2.5$ and the acceptance is given for events generated in different $p_T^{\rm hard}$ bins. Lepton reconstruction and b-tagging efficiencies are not included.

Cumulative acceptance	14 TeV pp (1)	2 TeV $p\bar{p}$ (2)	2 TeV $p\bar{p}$(*reduced*) (3)	Ratio (1)/(3)
	Zjj			
2 leptons	27.6%	56.2%	50.8%	0.54
+ 2 b-labelled jets	filter	filter	filter	—
+ jet veto 30 GeV	8.4%	24.8%	20.5%	0.41
	$t\bar{t}$			
2 leptons	2.6%	3.4%	3.2%	0.81
+ 2 b-labelled jets	1.6%	2.2%	1.9%	0.50
+ jet veto 30 GeV	0.7%	1.7%	1.5%	0.47

TABLE XXXII

Heavy flavour composition of Zjj events accepted in the mass window for jets with $p_T > 15$ GeV. No jet veto is applied.

Fraction in mass window	14 TeV pp	2 TeV $p\bar{p}$
bb	2.3%	1.0%
bc	0.2%	0.7%
cc	2.0%	1.2%
jb	5.5%	2.3%
jc	9.6%	6.2%
jj	80.4%	89.0%

3.3.3. Total signal and background

Table XXXIV compares the expected signal and backgrounds for the 14 TeV pp and the 2 TeV $p\bar{p}$ scenarios as estimated with and without jet-veto. For istance, assuming a comparable detector performance and no jet veto, the expected signal is 5.7 times higher and the total background 36 times higher for the 14 TeV pp. The significances are comparable in both cases, but the signal-to-background ratio is much larger for the 2 TeV $p\bar{p}$ scenario.

The estimates presented in Table XXXIV show that the sensitivity to this channel, is marginal for both scenarios. Also, in both cases the dominant background is $Zb\bar{b}$, which is underestimated in PYTHIA.

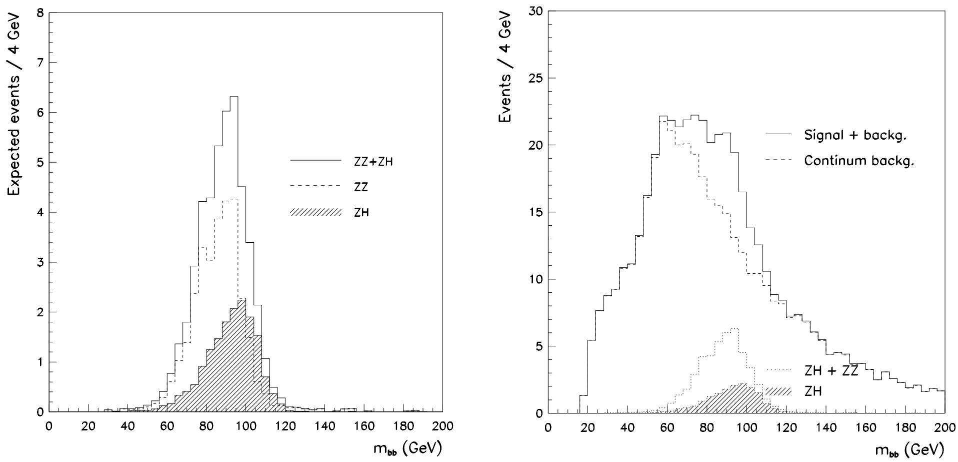

Fig. 7. The expected shape of the m_{bb} distributions for (left): signal, resonant background and signal plus backgorund and (right) continuum background and signal plus total background; for the Higgs mass of 100 GeV at 2 TeV $p\bar{p}$ collisions. A jet veto at 30 GeV is used and the plots are normalised to the expected number of events for an integrated luminosity of 30 fb^{-1}.

TABLE XXXIII

For an integrated luminosity of 30 fb^{-1}, expected number of events from the Zjj and $t\bar{t}$ backgrounds after all cuts. Acceptance inside the mass window, lepton reconstruction efficiency and b-tagging efficiency are included.

Expected events	14 TeV pp (1)	2 TeV $p\bar{p}$ (2)	2 TeV $p\bar{p}$ (reduced) (3)	Ratio (1)/(3)
	Zjj (bb)			
No jet-veto	8300	195	130	64
Jet-veto 30 GeV	6300	180	120	52
	Zjj (other)			
No jet-veto	700	20	14	50
Jet-veto 30 GeV	500	20	14	36
	$t\bar{t}$			
No jet veto	850	17	15	57
Jet veto 30 GeV	350	13	11	32

TABLE XXXIV

For an integrated luminosity of 30 fb^{-1}, expected numbers of signal and background events after all cuts.

Process	14 TeV pp (1)	2 TeV $p\bar{p}$ (2)	2 TeV $p\bar{p}$ (reduced) (3)	Ratio (1)/(3)
	No jet-veto			
ZH	115	20	18	6.4
ZZ	230	47	34	6.8
tt	850	17	15	57
Zjj (bb)	8300	195	130	64
Zjj (other)	700	20	14	50
Total bgd	10100	280	190	55
$S/\sqrt{B}$	1.1	1.2	1.3	0.8
S/B	1.1%	7.1%	9.5%	0.1
	Jet-veto 30 GeV			
ZH	80	16	15	5.3
ZZ	160	28	23	6.9
tt	350	13	11	32
Zjj (bb)	6300	180	120	52
Zjj (other)	500	20	14	36
Total bgd	7300	240	170	43
$S/\sqrt{B}$	0.9	1.0	1.1	0.8
S/B	1.1%	6.6%	8.8%	0.2

3.3.4. Comparison with the Tevatron report [2]

A direct comparison with the results presented in [2] is shown in Table XXXV. There is a clear disagreement in the predicted signal and backgrounds. For the results presented in the column *This study*, the ATLAS performance is assumed, but the selection criteria proposed in [2] are used. This includes smaller pseudorapidity coverage and softer jet veto, as already discussed in Section 3.3. The column *This study scaled* shows rates rescaled by a factor 1.7, obtained assuming the double b-tag acceptance for signal events as in the Tevatron study for the WH channel.

The discrepancy in the predicted signal rates is consistent with a factor of 2 higher effective acceptance for double b-tag including jet reconstruction for double b-tag and a factor 1.3 higher signal cross-section used by the Tevatron studies. Very significant is the discrepancy in the predicted rates for the dominant $Zb\bar{b}$ background. These are 3 times lower in the Tevatron study, even after taking into account the different double b-tag efficiency. A more detailed comparison is not possible for this channel as a break-down of the acceptances is not available [2].

TABLE XXXV

Comparison between "This study" (A), "This study scaled" (A') (see text) and the Tevatron report (B) (numbers are taken from Table 19 in Section C of [2]). The expected number of events is given for a 80–120 GeV mass window in "This study" and for 80–125 GeV mass window for Tevatron report.

Process	This study (A)	This study scaled (A')	Tevatron report (SHW study) (B)	Ratio (A)/(B)	Ratio (A')/(B)
ZH	15	25	36	0.4	0.7
ZZ	23	40	63	0.4	0.6
tt	11	20	57	0.2	0.3
Zbb	120	200	72	1.7	2.8
Zjj (other)	14	14	none	—	—
Total bgd	170	275	192	0.9	1.4
$S/\sqrt{B}$	0.8	1.4	2.6	0.3	0.5
S/B	6.5%	9.1%	18.7%	0.3	0.5
$B_{\text{other}}/B_{\text{total}}$	8%	5%	none	—	—

4. Conclusions

The primary aim of this paper was to understand the differences in the expected potential for the Higgs discovery in the WH/ZH, $H \to b\bar{b}$, $W/Z \to lepton(s)$ channels for 2 TeV $p\bar{p}$ and 14 TeV pp collisions. The aim was also to quantify, if possible, the origin of the differences in the expected discovery potential as estimated in [2] for 2 TeV $p\bar{p}$ collisions and in [1] for 14 TeV pp collisions.

As already stressed, the WH with $H \to b\bar{b}$ channel is not considered as a discovery channel at LHC.

It has been confirmed here that the overall sensitivity is below 4σ m_H= 100 GeV and around 2σ for m_H=120 GeV. This includes only the statistical errors and not possibly large systematic uncertainties coming from theoretical predictions and detector performance.

A detailed comparison of the expected signal and background for 14 TeV pp collisions and 2 TeV $p\bar{p}$ collisions was presented assuming the same detector performance and ATLAS-like or Tevatron-like selection criteria. The results obtained in this study for the 2 TeV $p\bar{p}$ scenario are much less promising than those reported in [2]. A direct comparison performed for $m_H = 110$ GeV shows that in [2] the signal rate is estimated to be 1.8 times higher and the background rates 1.7 times higher. This leads to a 1.3 times larger $S/\sqrt{B}$. The above discrepancy are roughly consistent with the assumed in [2] almost 1.7 times better effective efficiency for double b-tag than these so far established for ATLAS (with comparable or better rejection against non-b

jets) and with assumed factor 1.3 higher cross-section for the signal events and 1.3 lower acceptance for the jet-veto.

The sensitivity to the $\ell\ell b\bar{b}$ signature was evaluated here to be at the level of 1σ only for an integrated luminosity of 30 fb^{-1} and for both the 14 TeV pp and 2 TeV $p\bar{p}$ cases. As the selection does not require a tight jet-veto cut this channel could also be studied at high luminosity with a loss of performance due only to the reduced b-tagging capability. However, even with the ultimate integrated luminosity of 300 fb^{-1} the expected sensitivity would not exceed 3.0σ at LHC. An additional difficulty comes from the fact that the expected signal is only at the level of 30–50% of the resonant background.

A direct comparison shows that for $\ell\ell b\bar{b}$ final states the signal rates are estimated to be 2.4 times higher and the background rates 1.1 times higher in [2] than in the study shown here for 2 TeV $p\bar{p}$ collisions.

This work has been done in the framework of the ATLAS Collaboration, to which I am grateful for very valuable inputs and discussions.

In particular, it presents an extension and continuation of the previous study done with Daniel Froidevaux and documented in [3]. I would like to thank him very warmly for valuable suggestions and inspiring discussions which guided the present study. I am also grateful to Fabiola Gianotti and Karl Jakobs for several very constructive critical comments.

REFERENCES

[1] ATLAS Collaboration, ATLAS Detector and Physics Performance Technical Design Report, CERN/LHCC/99-14, ATLAS TDR 14, 25 May 1999.

[2] Report of the Physics at RUN II Supersymmetry/Higgs Workshop, Fermilab, 1999, eds. M. Carena and J. Lykken, in preparation, version 6, 25 June 2000.

[3] D. Froidevaux, E. Richter-Wąs, ATLAS Note ATL-PHYS-94-043 (1994), *Z. Phys.* **C67**, 213 (1995).

[4] ATLAS Collaboration, ATLAS Technical Proposal, CERN/LHCC/94-43, 15 December 1994.

[5] E. Richter-Wąs, *Acta Phys. Pol.* **B31**, 1973 (2000).

[6] E. Richter-Wąs, D. Froidevaux, L. Poggioli, ATLAS Note ATL-PHYS-98-131 (1998).

[7] ATLAS Collaboration, ATLAS Calorimeter Performance Technical Design Report, CERN/LHCC/96-40, 15 December 1996.

[8] ATLAS Collaboration, ATLAS Inner Detector Technical Design Report, CERN/LHCC/98-13.

[9] M.L. Mangano, *Nucl. Phys.* **B405**, 536 (1993).

[10] F.A. Berends, H. Kuijf, B. Tausk, W.T. Giele, *Nucl. Phys.* **B357**, 32 (1991); W. Giele, E. Glower, D. Kosower, *Nucl. Phys.* **B403**, 633 (1993).

[11] M.L. Mangano, P. Nason, *Phys. Lett.* **B285**, 160 (1992).

[12] M. Cobal, D. Costanzo, S. Lami, ATLAS Internal Note ATL-PHYS-96-084 (1996).

[13] S. Baranov, M. Smizanska, ATLAS Internal Note ATL-PHYS-98-133 (1998).

[14] B. Dick, Further work on WH, H $\rightarrow b\bar{b}$, ATLAS Communications, ATL-COM-PHYS-99-019 (1999).

[15] B. van Eijk, R. Kleiss, Proceedings of the Large Hadron Collider Workshop, Aachen, 1990, eds. Jarlskog and D. Rein, CERN 90-10/ECFA 90-133.

[16] *e.g.* J.Conway, Searching for the Higgs in Run 2 at the Tevatron, presentation on SUSY-99 Conference, Fermilab, June 14, 1999; M. Carena, Higgs Physics at Tevatron Collider, XXXIVnd Rencontres de Moriond, Les Arcs, France, on March 17, 1999; M.P.T. Roco, Prospects for the Higgs Discovery at the Tevatron, presented on EPS-HEP99, Tampere, Finland, 15 July 1999.

[17] J. Conway, Prospects for Higgs Searches at the Tevatron, talk given on the LHCC open session, CERN, 5 July 2000.